451-01-004 / 451-01-004 ISMRM ABSTRACT

Joint Optimization of Parallel Transmit RF Pulses and Gradient Waveforms for 2D Spatially Selective Excitation

PowerPitch Oral · 2 min + **Digital Poster** · 60 min | Parallel Transmission at High Fields · Tuesday, 12 May, 8:26 AM–8:28 AM · Session: 8:20–9:56 AM · Power Pitch Theatre 1 **Keywords:** MACHINE LEARNING/ARTIFICIAL INTELLIGENCE PARALLEL TRANSMIT & MULTIBAND RF PULSE DESIGN & FIELDS 7 TESLA MULTI-DIMENSIONAL SELECTIVE EXCITATION

Yuliang Xiao [1,2], **Jason Rock**[1,2], **Tim Zhe Wu**[3], **Jamie Near**[1,2], **Mark Chiew**[1,2], **Simon J Graham**[1,2]

[1]Physical Sciences Platform, Sunnybrook Research Institute, Toronto, Canada
[2]Department of Medical Biophysics, University of Toronto, Toronto, Canada
[3]Siemens Healthcare Limited, Montreal, Canada

Presenting Author: *Yuliang Xiao (yl.xiao@mail.utoronto.ca)*

Impact

Unifying multi-channel radiofrequency and gradient optimization within a self-supervised learning framework enables the design of high-fidelity spatially selective radiofrequency pulses. The proposed approach achieves precise excitation patterns, advancing the practicality of reduced field-of-view MRI for a wide range of applications.

Synopsis

Motivation: Previously, self-supervised two-dimensional radiofrequency pulse design has focused on single-channel transmit and fixed gradient waveforms, limiting spatial selectivity and fidelity. These restrictions hamper reduced field-of-view imaging for small, artifact-prone brain regions, such as the hippocampus, at ultra-high field.

Goals: To jointly optimize radiofrequency pulses and gradient waveforms, and incorporate parallel transmission for precise, robust region-of-interest two-dimensional selective excitation.

Approach: A physics-informed, self-supervised framework simultaneously optimizes multi-channel radiofrequency pulses and gradient waveforms via differentiable Bloch simulations, given B_1^+ and B_0 off-resonance maps and a target excitation mask.

Results: Phantom experiments show improved spatial selectivity, sidelobe suppression, and fidelity over single-channel and radiofrequency-only optimization.

Introduction

Designing radiofrequency (RF) pulses for two-dimensional (2D) spatially selective excitation remains challenging, especially for ultra-high field (UHF) MRI where field inhomogeneities and hardware limits degrade excitation accuracy[1]. The UHF scenario requires coordinated control of RF pulses and gradient waveforms to shape the excitation pattern within physical constraints, adopting parallel transmission (pTx) to exploit spatial degrees of freedom[2-4]. Recent self-supervised learning approaches have shown promise for RF design but are typically restricted to single-transmit (sTx) configurations with fixed gradient trajectories[5-8]. Here we introduce a self-supervised framework that jointly optimizes pTx RF and gradient waveforms enabling high-fidelity, spatially selective excitation and advancing the learning-based design of 2D selective pulses[9-11].

Methods

A physics-informed, self-supervised framework was developed for jointly optimizing pTx RF and gradient waveforms. The architecture (Fig. 1) consists of two main components: (a) a Feature Compression and Selection Module for simulation-based pre-training; and (b) a joint RF-gradient optimization network named *SelExNet*. In (a), principal component analysis (PCA)[12] and Gaussian mixture modeling (GMM)[13] were applied to the obtained B_0 / B_1^+ maps to acquire a low-dimensional embedding of field inhomogeneities. During training, the model randomly sampled B_0 / B_1^+ maps from this realistic distribution. In the *SelExNet*, an RF module predicted multi-channel RF pulses, while a Gradient module optimized parameterized spiral gradient waveforms. To further adapt the pretrained model to individuals, a transfer learning strategy was implemented. Subject-specific B_0 / B_1^+ maps were embedded as an additional conditioning input for individual fine-tuning.

A differentiable Bloch simulator enforced physics-consistent learning, with RF amplitude, gradient strength, and slew rate constraints incorporated as penalty terms. The total loss was defined as:

$$\mathcal{L}_{\text{total}} = \mathcal{L}_{\text{profile}} + \lambda_{\text{RF}}\mathcal{L}_{\text{RF}} + \lambda_{\text{Grad}}\mathcal{L}_{\text{Grad}} \qquad (1)$$

where $\mathcal{L}_{\text{profile}}$ enforces excitation fidelity, and $\mathcal{L}_{\text{RF}}$, $\mathcal{L}_{\text{Grad}}$ penalize RF power and gradient violations. λ_{RF} and λ_{Grad} are the constant coefficients to balance the weights for a smooth optimization process.

Evaluation: *SelExNet* was benchmarked against (1) fixed-gradient RF-only optimization; (2) sTx designs (CP mode); and (3) Spiral2D option in a 3D FLASH sequence from the Siemens-provided MATLAB Parallel Pulse Design Toolbox. Performance was assessed on simulated ROIs and phantom experiments using excitation fidelity, residual signal suppression, and spatial selectivity. All MRI experiements were performed with an 8ch pTx 7T MRI system (MAGNETOM Terra.X, Siemens Healthineers, Forchheim, Germany) using a spherical phantom filled with aqueous nickel sulfate hexahydrate.

Results

Fig. 2 compares RF-only (mono-optimization) with RF-gradient joint-optimization using the proposed framework. Mono-optimization with fixed gradients produced excitation profiles with significant sidelobes and reduced fidelity to the target mask in both simulation and experiment. In contrast, joint-optimization yielded excitation profiles that closely matched the target with substantially improved spatial selectivity and reduced off-target excitation. Quantitative metrics in Table 1 (Fig. 3) demonstrate increased excitation fidelity, lower normalized error, and improved background signal suppression for joint-optimization relative to RF-only mono-optimization.

Fig. 4 shows phantom experiments incorporating measured B_0 / B_1^+ maps. Pre-trained pulses showed nonuniformity and geometric distortion, whereas subject-specific fine-tuning restored target geometry, improved edge sharpness, and reduced background artifacts. These results confirm that fine-tuning enhances robustness to field inhomogeneities and subject-specific imperfections.

Fig. 5 compares results from vendor-provided dynamic pTx, *SelExNet* CP mode (analogous to sTx), and *SelExNet* full pTx mode implementations. Vendor-provided dynamic pTx yielded strong global excitation and background artifacts, demonstrating limited spatial confinement and nonuniform flip-angle distribution. *SelExNet* in CP mode improved excitation localization and reduced peripheral excitation, but residual intensity variation remained within the letters. The Full-mode *SelExNet* achieved the closest match to the target, producing uniform excitation, sharper boundaries, and minimal off-target signal.

Discussion

The proposed physics-informed, self-supervised framework jointly optimizes RF and gradient waveforms under pTx through differentiable Bloch simulations with hardware-aware constraints. The PCA-GMM-based sampling of B_0 / B_1^+ maps allows stochastic pre-training across realistic inhomogeneity distributions, enhancing robustness and generalization.

RF-gradient joint-optimization yields higher excitation fidelity, sharper edges, and lower sidelobe artifacts than fixed-gradient, RF-only methods. Incorporating pTx further improves uniformity and resilience to field variations, with full-mode *SelExNet* produces the most spatially confined and uniform excitation, outperforming both the on-scanner pTx and CP-mode configurations. These findings confirm that the proposed joint-optimization effectively leverages gradient and transmit-channel degrees of freedom for accurate, selective excitations enabling reduced field-of-view imaging.

Conclusion

This study presents *SelExNet*, a self-supervised, physics-informed framework for joint RF and gradient waveform optimization enabling 2D spatially selective excitation in UHF MRI. The method ensures hardware compliance and adapts to system- and subject-specific B_0 / B_1^+ variations. *SelExNet* provides a generalizable solution for high-resolution reduced field-of-view imaging and will be extended to 3D excitations with integrated dynamic motion and SAR constraints, facilitating rapid, subject-specific pulse optimization for clinical translation.

References

1. Williams SN, McElhinney P, Gunamony S. Ultra-high field MRI: parallel-transmit arrays and RF pulse design. Phys Med Biol. 2023;68(2):10.1088/1361-6560/aca4b7. doi:10.1088/1361-6560/aca4b7

2. Pauly J, Nishimura D, Macovski A. A k-space analysis of small-tip-angle excitation. 1989. J Magn Reson. 2011;213(2):544-557. doi:10.1016/j.jmr.2011.09.023

3. Grissom WA, Xu D, Kerr AB, Fessler JA, Noll DC. Fast large-tip-angle multidimensional and parallel RF pulse design in MRI. IEEE Trans Med Imaging. 2009;28(10):1548-1559. doi:10.1109/TMI.2009.2020064

4. Cloos MA, Boulant N, Luong M, et al. kT -points: short three-dimensional tailored RF pulses for flip-angle homogenization over an extended volume. Magn Reson Med. 2012;67(1):72-80. doi:10.1002/mrm.22978

5. Jang A, He X, Liu F. Physics-guided self-supervised learning: Demonstration for generalized RF pulse design. Magn Reson Med. 2025;93(2):657-672. doi:10.1002/mrm.30307

6. Bartlett JJ, Davey CE, Tyshchenko I, Blunck Y, Duan J, Johnston LA, Lévy S. Quasi-instantaneous subject-specific slice-by-slice pTx pulse design with Deep Learning: application to 2D diffusion MRI. Proc Int Soc Magn Reson Med. 2025.

7. Huang H, Yang Q, Wang J, Zhang P, Cai S, Cai C. High-efficient Bloch simulation of magnetic resonance imaging sequences based on deep learning. Phys Med Biol. 2023;68(8):10.1088/1361-6560/acc4a6. doi:10.1088/1361-6560/acc4a6

8. Loktyushin A, Herz K, Dang N, et al. MRzero - Automated discovery of MRI sequences using supervised learning. Magn Reson Med. 2021;86(2):709-724. doi:10.1002/mrm.28727

9. Zhang X, Pang Y. Parallel Excitation in Ultrahigh Field Human MR Imaging and Multi-Channel Transmit System. OMICS J Radiol. 2012;1(3):e110. doi:10.4172/2167-79641000e110

10. Zheng H, Zhao T, Qian Y, Schirda C, Ibrahim TS, Boada FE. Multi-slice parallel transmission three-dimensional tailored RF (PTX 3DTRF) pulse design for signal recovery in ultra high field functional MRI. J Magn Reson. 2013;228:37-44. doi:10.1016/j.jmr.2012.12.021

11. Davids M, Schad LR, Wald LL, Guérin B. Fast three-dimensional inner volume excitations using parallel transmission and optimized k-space trajectories. Magn Reson Med. 2016;76(4):1170-1182. doi:10.1002/mrm.26021

12. Abdi H, Williams LJ. Principal component analysis. Wiley Interdiscip Rev Comput Stat. 2010;2(4):433-459. doi:10.1002/wics.101

13. Rasmussen CE. The infinite Gaussian mixture model. Adv Neural Inf Process Syst. 1999;12:554-560. doi:10.5555/3009657.3009736

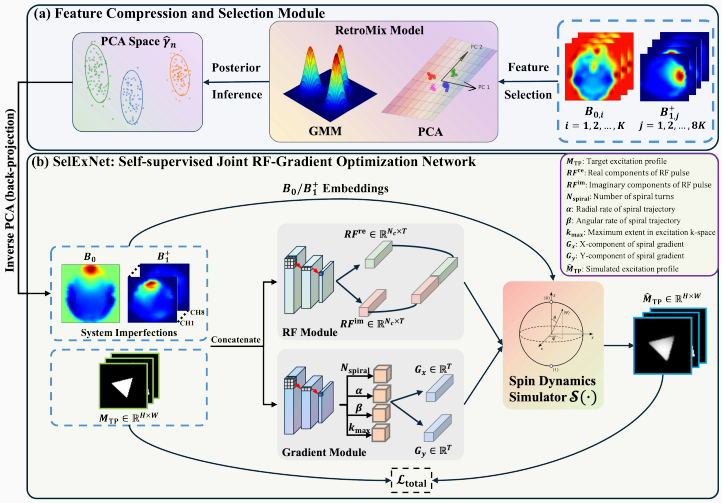

Scan for high-resolution version

Figure 1: *Overview of the self-supervised framework for joint RF and gradient pulse optimization: (a) Feature Compression and Section Module; (b) SelExNet network architecture. PCA and GMM extract statistical patterns from B_0/B_1^+ maps. N_c and T represent the number of transmit channels and time samples of RF and gradients waveforms, respectively. $H \times W$ is the excitation matrix size and $\mathcal{S}(\cdot)$ simulates spin dynamics via Bloch equations.*

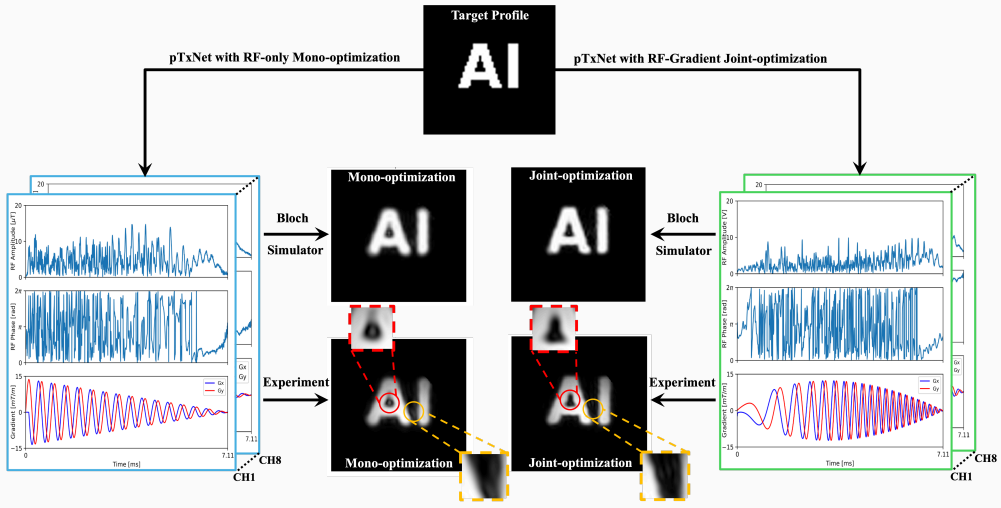

Scan for high-resolution version

Figure 2: *Comparison of mono- vs. joint-optimization for the "AI" target. Columns show the target profile, Bloch simulation, and experimental validation for RF-only and joint-optimized pulses. The zoomed-in region (inset) shows the mono-optimization introduces blurred edges and generates more signals at the gap between "A" and "I", whereas joint optimization achieves sharper strokes, improved uniformity, and lower background leakage.*

Table 1: Evaluation on the 2D spatially selective excitation

Algorithm	SSIM ↑	PSNR ↑	NRMSE ↓	BSR ↓
On-scanner pTx	0.653	18.6	0.182	0.157
SelExNet (Fixed G/CP mode)	0.937	26.2	0.053	0.016
SelExNet (Joint RF-G/CP mode)	0.956	27.6	0.042	0.012
SelExNet (Joint RF-G/pTx)	**0.964**	**28.5**	**0.037**	**0.007**

Scan for high-resolution version

Figure 3: *Quantification of 2D excitations between our and default on-scanner algorithms. BSR is the background-to-signal ratio used to evalute the performance of background signal suppression. It is defined by $\text{BSR} = \frac{\overline{|M_\mathrm{bg}|}}{\overline{|M_\mathrm{ROI}|}}$ where $\overline{|M_\mathrm{bg}|}$ and $\overline{|M_\mathrm{ROI}|}$ denote the mean excitation magnitude in the background and target regions, respectively.*

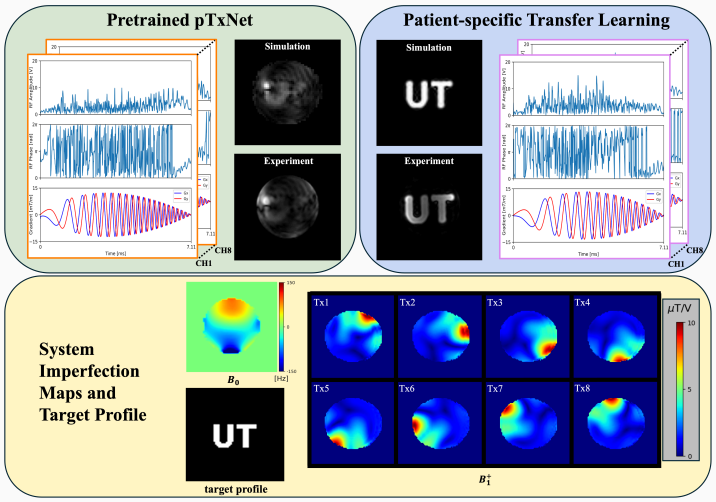

Scan for high-resolution version

Figure 4: *Phantom experiments with measured B_0/ B_1^{+} maps. Bottom: B_0/ B_1^{+} maps and target profile. Left and right: Bloch simulations and experimental results using pretrained pulses (left) and subject-specific finetuned pulses (right). Pre-trained pulses exhibit distortions and non-uniformity, whereas fine-tuned pulses restore the target geometry with improved edge sharpness and reduced background artifacts.*

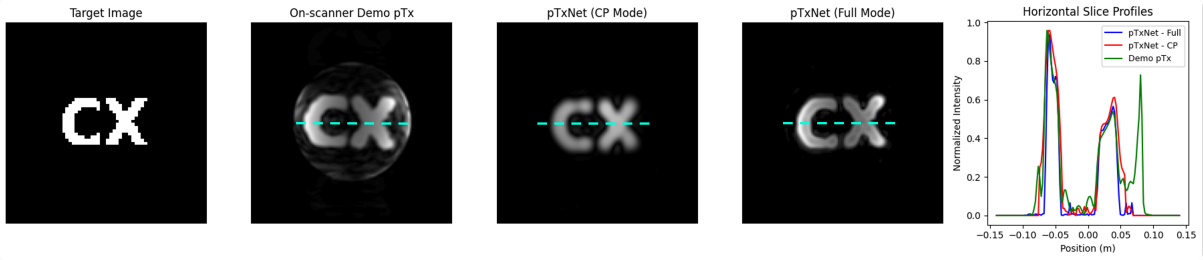

Scan for high-resolution version

Figure 5: *Comparison between vendor-provided demo pTx algorithm, SelExNet in CP-mode, and SelExNet in full pTx mode for the "CX" target. The demo pTx shows global excitation and background artifacts; CP mode improves confinement but reduced edge sharpness, whereas full-mode SelExNet best reproduces the target pattern with uniform intensity and minimal leakage, demonstrating the advantage of multi-channel joint optimization.*